Fisher-Information/CRLB Analyses for CF/m-MIMO-AP Jointly Optimized ISAC Networks

Xi Zhang and Guohao Pang
Networking and Information Systems Laboratory
Department of Electrical and Computer Engineering, Texas A&M University, College Station, TX 77843, USA
E-mail: {*xizhang@ece.tamu.edu*, *mikepang@tamu.edu*}

***Abstract*—Future 6G wireless systems are expected to provide not only high-rate communication but also reliable environment sensing through a unified air interface. Understanding the fundamental sensing limits in distributed architectures is therefore essential for guiding pilot design, array configuration, and resource allocation. We investigate sensing performance in an integrated sensing and communication (ISAC) cell-free massive MIMO network with distributed access points (APs) and a single mobile user. Under a Gaussian observation model, we derive an information-theoretic upper bound on the trace of the Fisher information matrix (FIM) by linking mutual information and the sub-Gaussian property of the score function. We obtain closed-form Cramér–Rao lower bounds (CRLBs) for estimating the real and imaginary parts of the channel gain and the angle of arrival (AoA), by exploiting the block-diagonal FIM structure and Schur-complement-based matrix inversion. Our derived CRLBs explicitly characterize how pilot length, noise variance, array size, and channel strength affect estimation accuracy. In particular, the AoA CRLB decreases with pilot length, received signal strength, and array aperture, while channel-gain CRLBs are mainly governed by pilot resources and noise level with additional coupling to angular parameters. These results provide analytical guidance for optimizing the pilot design and antenna configuration in cell-free ISAC sensing systems.**

I. Introduction

Integrated sensing and communication (ISAC) is a key technology for beyond-5G and 6G systems, enabling communication and sensing to share spectrum and hardware resources [1]. Cell-free massive MIMO further improves coverage and macro-diversity through distributed access points (APs) coordinated by a central processing unit (CPU) [2]. Their integration is therefore promising for high-accuracy networked sensing in spatially heterogeneous environments [3].

A central challenge is to characterize sensing accuracy under distributed reception and noisy pilot observations. Existing ISAC sensing studies often rely on specific estimators or simulation curves [4], while fewer works provide explicit information-theoretic limits that characterize the impact of pilot length, array geometry, noise, and channel strength [5]. In cell-free systems, AP-wise parameter coupling further complicates how local sensing information contributes to global estimation performance [6].

To overcome the above-mentioned difficulties, in this paper, we develop the Fisher-information and CRLB techniques for jointly optimizing cell-free massive-MIMO AP-based sensing accuracy over ISAC mobile networks. We derive an upper bound on the trace of the Fisher information matrix (FIM), connect it to mutual information and sub-Gaussian score functions, and obtain closed-form Cramér–Rao lower bounds (CRLBs) for channel-gain and angle-of-arrival (AoA) estimation. These results reveal how pilot resources, antenna number, array aperture, and signal-to-noise conditions affect sensing accuracy.

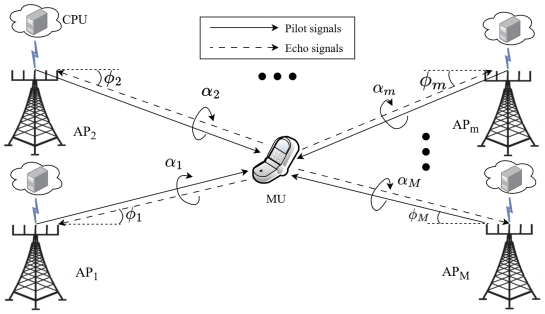

Fig. 1. The Fisher-information and CRLB model for joint-optimizing CF/m-MIMO-AP based ISAC mobile networks.

The rest of this paper is organized as follows. Section II presents the system model. Section III derives the Fisher-information bound and CRLB results. Section IV develops the joint multiple-resource optimization scheme. Section V evaluates performances, and Section VI concludes the paper.

Notation: $[\cdot]^{\mathsf{T}}$, $\|\cdot\|_2$, $\mathbf{I}_N$, $\mathbb{E}[\cdot]$, $\mathrm{vec}(\cdot)$, $\exp(\cdot)$, $\lambda_{\max}(\cdot)$, $\Re\{\cdot\}$, $\mathrm{Cov}(\cdot)$, and $[\mathbf{A}]_{i,j}$ denote transpose, Euclidean norm, identity matrix, expectation, vectorization, exponential function, largest eigenvalue, real part, covariance, and the (i,j)-th matrix entry, respectively. For symmetric matrices, $\mathbf{A} \succeq \mathbf{B}$ means that $\mathbf{A} - \mathbf{B}$ is positive semidefinite.

II. The System Models

A. Network Model

We consider an ISAC cell-free massive MIMO network with M APs, each equipped with L antennas, serving a single-antenna MU at $\boldsymbol{\rho} = [\rho_x, \rho_y]^{\mathsf{T}} \in \mathbb{R}^2$. The AP and antenna index sets are $\mathcal{M} = \{1, \ldots, M\}$ and $\mathcal{L} = \{1, \ldots, L\}$, respectively. Pilot symbols are used for sensing, and each pilot has length T with pilot-time index set $\mathcal{T}_{\mathrm{p}} = \{1, \ldots, T\}$. The noise variance is σ^2. For AP $m \in \mathcal{M}$, define $\boldsymbol{\theta}_m = [\alpha_{m,R}, \alpha_{m,I}, \phi_m]^{\mathsf{T}} \in \mathbb{R}^{3\times 1}$, where $\alpha_m = \alpha_{m,R} + j\alpha_{m,I}$ and ϕ_m is the AoA. The CPU collects the global real-valued parameter vector

$\Theta = \left[\boldsymbol{\theta}_1^{\mathsf{T}}, \ldots, \boldsymbol{\theta}_M^{\mathsf{T}}\right]^{\mathsf{T}} \in \mathbb{R}^{3M\times 1}$. The unit-norm ULA steering vector is

$$\mathbf{a}_m(\phi_m) = \frac{1}{\sqrt{L}}\left[1, e^{j\kappa \sin\phi_m}, \ldots, e^{j\kappa(L-1)\sin\phi_m}\right]^{\mathsf{T}}, \quad (1)$$

where $\kappa = 2\pi d/\lambda$, with antenna spacing d and wavelength λ. Let $s_{m,t}$ denote the t-th pilot of AP m, with $\mathbb{E}\left[|s_{m,t}|^2\right] = 1$. The received signal is

$$\mathbf{x}_{m,t} = \alpha_m \mathbf{a}_m(\phi_m) s_{m,t} + \mathbf{n}_{m,t}, \quad (2)$$

where $\mathbf{n}_{m,t} \sim \mathcal{CN}(\mathbf{0}, \sigma^2 \mathbf{I}_L)$. Stacking the T pilots at AP m gives

$$\mathbf{X}_m = [\mathbf{x}_{m,1}, \ldots, \mathbf{x}_{m,T}] = \alpha_m \mathbf{a}_m(\phi_m)\mathbf{s}_m + \mathbf{N}_m \in \mathbb{C}^{L\times T}, \quad (3)$$

where $\mathbf{s}_m = [s_{m,1}, \ldots, s_{m,T}]$ and $\mathbf{N}_m = [\mathbf{n}_{m,1}, \ldots, \mathbf{n}_{m,T}]$. The CPU observation is $\mathbf{x}_{\mathrm{C}} = \mathrm{vec}\left([\mathbf{X}_1, \ldots, \mathbf{X}_M]\right) \in \mathbb{C}^{MLT\times 1}$, and $\mathbf{s}_{\mathrm{C}} = [\mathbf{s}_1, \ldots, \mathbf{s}_M]$ collects all pilot sequences.

B. Fisher Information Model

Under i.i.d. Gaussian noise, the likelihood of $\mathbf{x}_{\mathrm{C}}$ is [7]

$$p\left(\mathbf{x}_{\mathrm{C}} \mid \Theta\right) = \prod_{m=1}^{M}\prod_{t=1}^{T} \frac{1}{\left(\pi\sigma^2\right)^L} \times \exp\left(-\frac{1}{\sigma^2}\left\|\mathbf{x}_{m,t} - \alpha_m \mathbf{a}_m(\phi_m) s_{m,t}\right\|_2^2\right). \quad (4)$$

Ignoring constants, taking the logarithm of the likelihood gives

$$\ell\left(\Theta; \mathbf{x}_{\mathrm{C}}\right) \triangleq \log p\left(\mathbf{x}_{\mathrm{C}} \mid \Theta\right) = -\frac{1}{\sigma^2}\sum_{m=1}^{M}\sum_{t=1}^{T}\left\|\mathbf{x}_{m,t} - \alpha_m \mathbf{a}_m(\phi_m) s_{m,t}\right\|_2^2. \quad (5)$$

Based on this log-likelihood, define the FIM with respect to the real parameter vector Θ as

$$\mathbf{I}_{\mathbf{x}_{\mathrm{C}}}(\Theta) = \mathbb{E}_{\mathbf{x}_{\mathrm{C}}|\Theta}\left[\nabla_\Theta \ell\left(\Theta; \mathbf{x}_{\mathrm{C}}\right) \nabla_\Theta^{\mathsf{T}} \ell\left(\Theta; \mathbf{x}_{\mathrm{C}}\right)\right]. \quad (6)$$

The mutual information between $\mathbf{x}_{\mathrm{C}}$ and $\mathbf{s}_{\mathrm{C}}$ is defined as

$$\mathcal{I}_\Theta\left(\mathbf{x}_{\mathrm{C}}; \mathbf{s}_{\mathrm{C}}\right) = \mathbb{E}_{\mathbf{x}_{\mathrm{C}}, \mathbf{s}_{\mathrm{C}}|\Theta}\left[\log \frac{p\left(\mathbf{x}_{\mathrm{C}}, \mathbf{s}_{\mathrm{C}}|\Theta\right)}{p\left(\mathbf{x}_{\mathrm{C}}|\Theta\right) p\left(\mathbf{s}_{\mathrm{C}}\right)}\right]. \quad (7)$$

Define the residual

$$\mathbf{r}_{m,t}(\boldsymbol{\theta}_m) = \mathbf{x}_{m,t} - \alpha_m \mathbf{a}_m(\phi_m) s_{m,t}. \quad (8)$$

At the true parameter $\boldsymbol{\theta}_m^*$, $\mathbf{r}_{m,t}(\boldsymbol{\theta}_m^*) = \mathbf{n}_{m,t}$. For $\alpha_{m,R}$,

$$\frac{\partial}{\partial \alpha_{m,R}}\left(\alpha_m \mathbf{a}_m(\phi_m) s_{m,t}\right) = \mathbf{a}_m(\phi_m) s_{m,t}. \quad (9)$$

Hence,

$$S_{\alpha_{m,R}}(\boldsymbol{\theta}_m) = \frac{\partial \ell\left(\Theta; \mathbf{x}_{\mathrm{C}}\right)}{\partial \alpha_{m,R}} = \frac{2}{\sigma^2}\sum_{t=1}^{T}\Re\left\{\left(\mathbf{a}_m(\phi_m) s_{m,t}\right)^{\mathsf{H}} \mathbf{r}_{m,t}(\boldsymbol{\theta}_m)\right\}. \quad (10)$$

At $\boldsymbol{\theta}_m = \boldsymbol{\theta}_m^*$,

$$S_{\alpha_{m,R}}(\boldsymbol{\theta}_m^*) = \frac{2}{\sigma^2}\sum_{t=1}^{T}\Re\left\{\left(\mathbf{a}_m(\phi_m) s_{m,t}\right)^{\mathsf{H}} \mathbf{n}_{m,t}\right\}, \quad (11)$$

which is real Gaussian. Likewise,

$$\frac{\partial}{\partial \alpha_{m,I}}\left(\alpha_m \mathbf{a}_m(\phi_m) s_{m,t}\right) = j\mathbf{a}_m(\phi_m) s_{m,t}, \quad (12)$$

with score function:

$$S_{\alpha_{m,I}}(\boldsymbol{\theta}_m) = \frac{2}{\sigma^2}\sum_{t=1}^{T}\Re\left\{-j\left(\mathbf{a}_m(\phi_m) s_{m,t}\right)^{\mathsf{H}} \mathbf{r}_{m,t}(\boldsymbol{\theta}_m)\right\}. \quad (13)$$

At $\boldsymbol{\theta}_m = \boldsymbol{\theta}_m^*$, $S_{\alpha_{m,I}}(\boldsymbol{\theta}_m^*)$ is also real Gaussian. For ϕ_m,

$$\frac{\partial}{\partial \phi_m}\left(\alpha_m \mathbf{a}_m(\phi_m) s_{m,t}\right) = \alpha_m \mathbf{a}_m'(\phi_m) s_{m,t}, \quad (14)$$

where $\mathbf{a}_m'(\phi_m) = \frac{\partial \mathbf{a}_m(\phi_m)}{\partial \phi_m}$. The corresponding score is

$$S_{\phi_m}(\boldsymbol{\theta}_m) = \frac{\partial \ell\left(\Theta; \mathbf{x}_{\mathrm{C}}\right)}{\partial \phi_m} = \frac{2}{\sigma^2}\sum_{t=1}^{T}\Re\left\{\left(\alpha_m \mathbf{a}_m'(\phi_m) s_{m,t}\right)^{\mathsf{H}} \mathbf{r}_{m,t}(\boldsymbol{\theta}_m)\right\}. \quad (15)$$

At $\boldsymbol{\theta}_m = \boldsymbol{\theta}_m^*$,

$$S_{\phi_m}(\boldsymbol{\theta}_m^*) = \frac{2}{\sigma^2}\sum_{t=1}^{T}\Re\left\{\left(\alpha_m \mathbf{a}_m'(\phi_m) s_{m,t}\right)^{\mathsf{H}} \mathbf{n}_{m,t}\right\}, \quad (16)$$

so $S_{\phi_m}(\boldsymbol{\theta}_m^*)$ is real Gaussian. Therefore,

$$\mathbf{S}_m(\boldsymbol{\theta}_m) = \left[S_{\alpha_{m,R}}(\boldsymbol{\theta}_m),\ S_{\alpha_{m,I}}(\boldsymbol{\theta}_m),\ S_{\phi_m}(\boldsymbol{\theta}_m)\right]^{\mathsf{T}} \quad (17)$$

is jointly Gaussian at $\boldsymbol{\theta}_m^*$. Hence, for any unit vector $\mathbf{u}$, $\mathbf{u}^{\mathsf{T}}\mathbf{S}_m(\boldsymbol{\theta}_m^*)$ is Gaussian, so $\mathbf{S}_m(\boldsymbol{\theta}_m^*)$ is sub-Gaussian with parameter N [8]. A zero-mean scalar random variable X_m is sub-Gaussian with parameter N if

$$\mathbb{E}\left[e^{\lambda X_m}\right] \le e^{\frac{\lambda^2 N^2}{2}} \quad (18)$$

for all $\lambda \in \mathbb{R}$ [9].

III. Fisher Information Bound and CRLB Analysis

A. Fisher Information Matrix

The FIM measures how sensitively the received pilot observations change with the sensing parameters. A larger FIM generally implies more accurate parameter estimation. However, the trace of the FIM alone does not clearly show how communication resources, such as pilot length and quantization bits, affect sensing accuracy. To make this relationship explicit, we upper-bound the FIM trace by using the mutual information $\mathcal{I}_\Theta(\mathbf{x}_{\mathrm{C}}; \mathbf{s}_{\mathrm{C}})$ between the CPU observation $\mathbf{x}_{\mathrm{C}}$ and the pilot sequence $\mathbf{s}_{\mathrm{C}}$. The following theorem therefore relates to the sensing-information bound to the pilot resources, channel strength, antenna number, and array geometry.

Theorem 1: **If** $\mathbf{I}_{\mathbf{x}_\mathrm{C}}(\Theta)$ is defined by Eq. (6) and $\mathcal{I}_\Theta\left(\mathbf{x}_\mathrm{C};\mathbf{s}_\mathrm{C}\right)$ is defined by Eq. (7), and their responding control parameters are defined as follows:

$$\begin{cases} |\alpha| \triangleq \max\limits_{m\in\mathcal{M}} |\alpha_m|\,, \\ \|\mathbf{a}'(\phi)\|_2 \triangleq \max\limits_{m\in\mathcal{M}} \|\mathbf{a}'_m(\phi_m)\|_2\,, \\ \cos^2\phi \triangleq \max\limits_{m\in\mathcal{M}} \cos^2\phi_m, \end{cases} \tag{19}$$

then the following claims hold:

Claim 1. Under the Gaussian observation model,

$$\mathsf{Tr}\left(\mathbf{I}_{\mathbf{x}_\mathrm{C}}(\Theta)\right) \le \frac{4MT}{\sigma^2}\left(2+|\alpha|^2\left\|\mathbf{a}'(\phi)\right\|_2^2\right)\mathcal{I}_\Theta\left(\mathbf{x}_\mathrm{C};\mathbf{s}_\mathrm{C}\right), \tag{20}$$

Claim 2. If $\mathbf{S}_m(\boldsymbol{\theta}_m)$ given by Eq (17) is sub-Gaussian with parameter N, and the number of L antennas is given, then

$$\mathsf{Tr}\left(\mathbf{I}_{\mathbf{x}_\mathrm{C}}(\Theta)\right) \le \frac{4MT}{\sigma^2}\mathcal{I}_\Theta\left(\mathbf{x}_\mathrm{C};\mathbf{s}_\mathrm{C}\right) \times\left(2+|\alpha|^2\kappa^2\left(\cos^2\phi\right)\frac{(L-1)(2L-1)}{6}\right), \tag{21}$$

Claim 3. If the total number b of bits contained by each pilot is given, then

$$\mathsf{Tr}\left(\mathbf{I}_{\mathbf{x}_\mathrm{C}}(\Theta)\right) \le \frac{8bT^2M^2L}{\sigma^2} \times\left(2+|\alpha|^2\kappa^2\left(\cos^2\phi\right)\frac{(L-1)(2L-1)}{6}\right). \tag{22}$$

Proof: The proof is provided in Appendix A [10], whose full version of this paper is available online. ∎

B. Overall CRLB Derived from the Trace Bound

Using the global parameter-vector ordering defined in Section II,

$$\Theta = \left[\alpha_{1,R},\alpha_{1,I},\phi_1,\ldots,\alpha_{M,R},\alpha_{M,I},\phi_M\right]^\mathsf{T} \in \mathbb{R}^{3M\times 1}. \tag{23}$$

For any unbiased estimator $\widehat{\Theta}$, the CRLB is [11]

$$\mathrm{Cov}(\widehat{\Theta}) \succeq \mathbf{I}_{\mathbf{x}_\mathrm{C}}(\Theta)^{-1}, \tag{24}$$

where $\mathbf{I}_{\mathbf{x}_\mathrm{C}}(\Theta)$ is the FIM of $\mathbf{x}_\mathrm{C}$. Taking traces gives [12]

$$\mathsf{Tr}\Big(\mathrm{Cov}(\widehat{\Theta})\Big) \ge \mathsf{Tr}\big(\mathbf{I}_{\mathbf{x}_\mathrm{C}}(\Theta)^{-1}\big)\,. \tag{25}$$

Let the eigenvalues of $\mathbf{I}_{\mathbf{x}_\mathrm{C}}(\Theta)$ be $\{\lambda_i\}_{i=1}^{3M}$ with $\lambda_i > 0$. Then

$$\mathsf{Tr}(\mathbf{I}_{\mathbf{x}_\mathrm{C}}(\Theta)) = \sum_{i=1}^{3M}\lambda_i, \text{ and } \mathsf{Tr}\big(\mathbf{I}_{\mathbf{x}_\mathrm{C}}(\Theta)^{-1}\big) = \sum_{i=1}^{3M}\frac{1}{\lambda_i}. \tag{26}$$

By Cauchy–Schwarz,

$$\left(\sum_{i=1}^{3M}\lambda_i\right)\left(\sum_{i=1}^{3M}\frac{1}{\lambda_i}\right) \ge 9M^2, \tag{27}$$

which implies

$$\mathsf{Tr}\big(\mathbf{I}_{\mathbf{x}_\mathrm{C}}(\Theta)^{-1}\big) \ge \frac{9M^2}{\mathsf{Tr}(\mathbf{I}_{\mathbf{x}_\mathrm{C}}(\Theta))}. \tag{28}$$

Hence,

$$\mathsf{Tr}\Big(\mathrm{Cov}(\widehat{\Theta})\Big) \ge \frac{9M^2}{\mathsf{Tr}(\mathbf{I}_{\mathbf{x}_\mathrm{C}}(\Theta))}. \tag{29}$$

Combining Eq. (29) with Eq. (22) derived in **Claim 3** of Theorem 1, and using the unbiased-estimator identity between total MSE and covariance trace, we obtain the following expression:

$$\mathbb{E}\left[\left\|\widehat{\Theta}-\Theta\right\|_2^2\right] = \mathsf{Tr}\Big(\mathrm{Cov}(\widehat{\Theta})\Big) \ge \frac{9\sigma^2}{8bT^2L\Big(2+|\alpha|^2\kappa^2\left(\cos^2\phi\right)\frac{(L-1)(2L-1)}{6}\Big)}. \tag{30}$$

C. CRLBs for Channel Gain and AoA

Independence across APs yields the block-diagonal FIM

$$\mathbf{I}_{\mathbf{x}_\mathrm{C}}(\Theta) = \begin{bmatrix} \mathbf{I}_1(\boldsymbol{\theta}_1) & \mathbf{0} & \cdots & \mathbf{0} \\ \mathbf{0} & \mathbf{I}_2(\boldsymbol{\theta}_2) & \cdots & \mathbf{0} \\ \vdots & \vdots & \ddots & \vdots \\ \mathbf{0} & \mathbf{0} & \cdots & \mathbf{I}_M(\boldsymbol{\theta}_M) \end{bmatrix}, \tag{31}$$

where $\mathbf{I}_m(\boldsymbol{\theta}_m) \in \mathbb{R}^{3\times 3}$ is the local FIM. Hence,

$$\mathrm{Cov}(\widehat{\Theta}) \succeq \begin{bmatrix} \mathbf{I}_1(\boldsymbol{\theta}_1)^{-1} & \mathbf{0} & \cdots & \mathbf{0} \\ \mathbf{0} & \mathbf{I}_2(\boldsymbol{\theta}_2)^{-1} & \cdots & \mathbf{0} \\ \vdots & \vdots & \ddots & \vdots \\ \mathbf{0} & \mathbf{0} & \cdots & \mathbf{I}_M(\boldsymbol{\theta}_M)^{-1} \end{bmatrix}. \tag{32}$$

Therefore, it suffices to invert each local FIM. Define

$$\begin{cases} q_m \triangleq \mathbf{a}_m(\phi_m)^\mathsf{H}\mathbf{a}'_m(\phi_m), \\ \eta_m \triangleq \|\mathbf{a}'_m(\phi_m)\|_2^2\,, \end{cases} \tag{33}$$

and

$$c_m \triangleq \kappa\left(\cos\phi_m\right)\frac{L-1}{2}. \tag{34}$$

Using the ULA steering-vector identities and the local Gaussian FIM, we obtain

$$\xi_m \triangleq |\alpha_m|^2(\eta_m - c_m^2) = |\alpha_m|^2\kappa^2\left(\cos^2\phi_m\right)\frac{L^2-1}{12}, \tag{35}$$

and the local FIM

$$\mathbf{I}_m(\boldsymbol{\theta}_m) = \frac{2T}{\sigma^2}\begin{bmatrix} 1 & 0 & -c_m\alpha_{m,I} \\ 0 & 1 & c_m\alpha_{m,R} \\ -c_m\alpha_{m,I} & c_m\alpha_{m,R} & |\alpha_m|^2\eta_m \end{bmatrix}. \tag{36}$$

Applying the Schur complement [13] to Eq. (36) yields

$$\mathbf{I}_m(\boldsymbol{\theta}_m)^{-1} = \frac{\sigma^2}{2T}\begin{bmatrix} 1+\frac{c_m^2\alpha_{m,I}^2}{\xi_m} & -\frac{c_m^2\alpha_{m,R}\alpha_{m,I}}{\xi_m} & \frac{c_m\alpha_{m,I}}{\xi_m} \\ -\frac{c_m^2\alpha_{m,R}\alpha_{m,I}}{\xi_m} & 1+\frac{c_m^2\alpha_{m,R}^2}{\xi_m} & -\frac{c_m\alpha_{m,R}}{\xi_m} \\ \frac{c_m\alpha_{m,I}}{\xi_m} & -\frac{c_m\alpha_{m,R}}{\xi_m} & \frac{1}{\xi_m} \end{bmatrix}. \tag{37}$$

The diagonal entries first give

$$\begin{cases} \mathrm{Var}(\widehat{\alpha}_{m,R}) \geq \dfrac{\sigma^2}{2T}\left(1+\dfrac{c_m^2\alpha_{m,I}^2}{\xi_m}\right), \\ \mathrm{Var}(\widehat{\alpha}_{m,I}) \geq \dfrac{\sigma^2}{2T}\left(1+\dfrac{c_m^2\alpha_{m,R}^2}{\xi_m}\right), \end{cases} \tag{38}$$

and

$$\mathrm{Var}(\widehat{\phi}_m) \geq \left[\mathbf{I}_m(\boldsymbol{\theta}_m)^{-1}\right]_{3,3} = \frac{\sigma^2}{2T\xi_m}. \tag{39}$$

Substituting Eq. (34) and Eq. (35) into Eq. (38) and Eq. (39) gives the following theorem.

Theorem 2: For the local parameter vector $\boldsymbol{\theta}_m = [\alpha_{m,R}, \alpha_{m,I}, \phi_m]^{\mathsf{T}}$, if $\alpha_m \neq 0$ and $\cos\phi_m \neq 0$, then the closed-form channel-gain CRLBs are

$$\begin{cases} \mathrm{Var}(\widehat{\alpha}_{m,R}) \geq \dfrac{\sigma^2}{2T}\left(1+\dfrac{3(L-1)}{L+1}\dfrac{\alpha_{m,I}^2}{|\alpha_m|^2}\right), \\ \mathrm{Var}(\widehat{\alpha}_{m,I}) \geq \dfrac{\sigma^2}{2T}\left(1+\dfrac{3(L-1)}{L+1}\dfrac{\alpha_{m,R}^2}{|\alpha_m|^2}\right), \end{cases} \tag{40}$$

and the closed-form AoA CRLB is

$$\mathrm{Var}(\widehat{\phi}_m) \geq \frac{6\sigma^2}{T\,|\alpha_m|^2\,\kappa^2\,(\cos^2\phi_m)\,(L^2-1)}. \tag{41}$$

Proof: The proof is provided in Appendix B [10]. ∎

Thus, the channel-gain bounds are mainly governed by T and σ^2, while the AoA error decreases with T, $|\alpha_m|^2$, and array aperture.

IV. Joint Multiple Resources Optimization Scheme

Define the AP-wise sensing-quality coefficient

$$g_m = |\alpha_m|^2 \cos^2\phi_m, \tag{42}$$

which combines channel strength and angular sensitivity. Sort the $M_{\max}$ candidate APs as

$$g_{(1)} \geq g_{(2)} \geq \cdots \geq g_{(M_{\max})}. \tag{43}$$

The accumulated gain of the best M APs is

$$G_M = \sum_{i=1}^{M} g_{(i)}. \tag{44}$$

The network-level AoA Fisher information is

$$I_\phi^{\mathrm{net}}(T,L,M) = \frac{T\kappa^2(L^2-1)}{6\sigma^2} G_M. \tag{45}$$

The corresponding CRLB is

$$\mathrm{CRLB}_\phi^{\mathrm{net}}(T,L,M) = \frac{6\sigma^2}{T\kappa^2(L^2-1)G_M}. \tag{46}$$

Balancing CRLB reduction with pilot overhead, AP activation, and antenna energy and number of antennas gives

$$J(T,L,M) = \frac{6\sigma^2}{T\kappa^2(L^2-1)G_M} + \beta\frac{T}{T_c} + \mu\frac{M}{M_{\max}} + \nu\frac{ML}{N_{\max}}, \tag{47}$$

where T_c is the coherence-block length, $N_{\max}$ is the antenna budget, and β, μ, and ν are cost weights.

The resulting problem is

$$\begin{aligned} \min_{T,L,M} \quad & J(T,L,M) \\ \text{s.t.} \quad & T_{\min} \leq T \leq T_{\max}, \\ & L_{\min} \leq L \leq L_{\max}, \\ & 1 \leq M \leq M_{\max}, \\ & ML \leq N_{\max}, \\ & T, L, M \in \mathbb{Z}^+. \end{aligned} \tag{48}$$

We solve this finite mixed-integer problem by alternating search. For fixed M and L, define

$$A_{M,L} = \frac{6\sigma^2}{\kappa^2(L^2-1)G_M}. \tag{49}$$

The function of T is

$$J_T(T) = \frac{A_{M,L}}{T} + \beta\frac{T}{T_c}. \tag{50}$$

The pilot-size update is

$$T^{(r+1)} = \arg\min_{T\in\mathcal{T}_{\mathrm{f}}} \left[\frac{A_{M^{(r)},L^{(r)}}}{T} + \beta\frac{T}{T_c}\right], \tag{51}$$

where

$$\mathcal{T}_{\mathrm{f}} = \left\{T \in \mathbb{Z}^+ \mid T_{\min} \leq T \leq T_{\max}\right\}. \tag{52}$$

The continuous reference solution is

$$T_0^\star(M,L) = \sqrt{\frac{A_{M,L}T_c}{\beta}}. \tag{53}$$

Then search $\mathcal{T}_{\mathrm{f}}$ for the integer $T^{(r+1)}$. The antenna-number update is

$$L^{(r+1)} = \arg\min_{L\in\mathcal{L}_{\mathrm{f}}(M^{(r)})} \left[\frac{6\sigma^2}{T^{(r+1)}\kappa^2\big(L^2-1\big)G_{M^{(r)}}} + \nu\frac{M^{(r)}L}{N_{\max}}\right], \tag{54}$$

with feasible set

$$\mathcal{L}_{\mathrm{f}}(M) = \left\{L \in \mathbb{Z}^+ \mid L_{\min} \leq L \leq L_{\max},\ ML \leq N_{\max}\right\}. \tag{55}$$

This balances array gain and antenna cost. The AP-number update is

$$M^{(r+1)} = \arg\min_{M\in\mathcal{M}_{\mathrm{f}}(L^{(r+1)})} \left[\frac{6\sigma^2}{T^{(r+1)}\kappa^2\big((L^{(r+1)})^2-1\big)G_M} + \mu\frac{M}{M_{\max}} + \nu\frac{ML^{(r+1)}}{N_{\max}}\right], \tag{56}$$

with feasible set

$$\mathcal{M}_{\mathrm{f}}(L) = \left\{M \in \mathbb{Z}^+ \mid 1 \leq M \leq M_{\max},\ ML \leq N_{\max}\right\}. \tag{57}$$

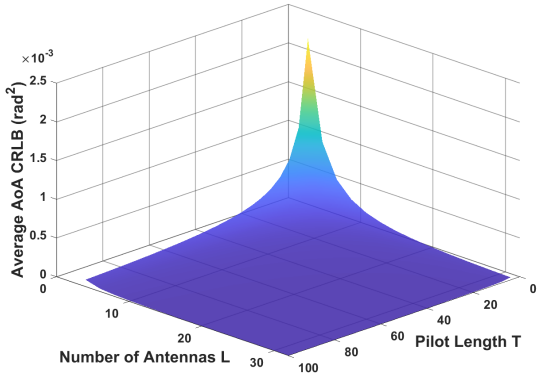

Fig. 2. The average AoA CRLB as a function of the pilot length T and the number of antennas L.

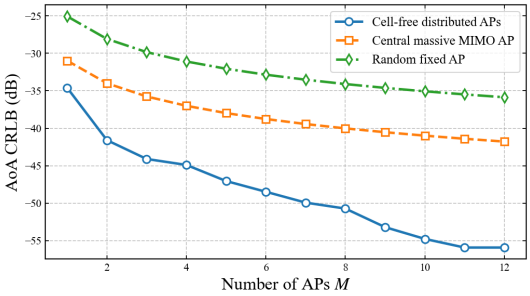

Fig. 3. Comparison of AoA CRLB versus the number of APs.

Thus, M trades accumulated sensing gain against activation and antenna-related costs.

Starting from feasible $\left(T^{(0)}, L^{(0)}, M^{(0)}\right)$, cyclically update T, L, and M until

$$\left| J\left(T^{(r+1)}, L^{(r+1)}, M^{(r+1)}\right) - J\left(T^{(r)}, L^{(r)}, M^{(r)}\right) \right| \leq \epsilon, \tag{58}$$

where ϵ is the tolerance. The final allocation is

$$(T^\star, L^\star, M^\star) = \left(T^{(r+1)}, L^{(r+1)}, M^{(r+1)}\right). \tag{59}$$

Hence, the selected configuration balances sensing accuracy and resource cost rather than maximizing T, L, or M alone.

V. Performances Evaluations

Fig. 2 shows the average AoA CRLB versus the pilot length T and the antenna number L. The CRLB decreases as T and L increase, and the strong gain from larger arrays is consistent with the scaling law $\text{CRLB} \propto 1/(TL^2)$. This highlights the importance of pilot allocation and antenna deployment in ISAC cell-free Massive MIMO sensing.

Fig. 3 compares the AoA CRLB of different deployments versus the number of APs. The distributed cell-free deployment gives the lowest CRLB, benefiting from shorter access distances and more favorable AoA geometry, while centralized and random fixed-BS deployments are limited by fixed geometry or larger path loss. This confirms the sensing advantage of distributed AP deployment.

Fig. 4 shows the sensing utility versus the number of activated APs under different antenna configurations, with T optimized for each (M, L) pair. Increasing M first improves

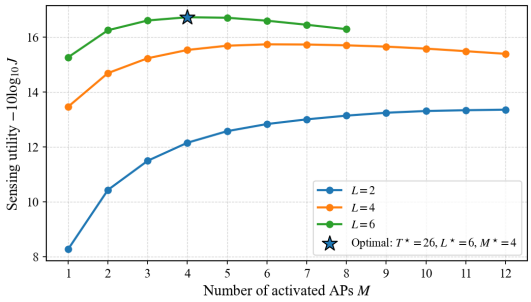

Fig. 4. Sensing utility function versus number of APs.

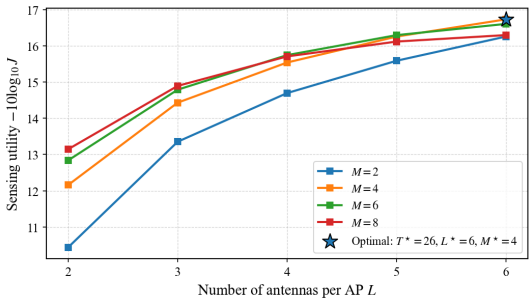

Fig. 5. Sensing utility function versus number of antennas per AP.

utility by accumulating Fisher information, but activation and RF-chain costs eventually cause saturation or degradation. Thus, activating all APs is not always optimal.

Fig. 5 shows the sensing utility versus the number of antennas per AP. A larger L improves array aperture and angular sensing, but the gain is limited by antenna/RF-chain cost. The proposed method therefore balances CRLB reduction and resource consumption instead of simply maximizing M or L.

VI. Conclusions

We developed a Fisher-information-based analytical framework for ISAC cell-free massive MIMO sensing and derived explicit CRLB expressions for channel-gain and AoA estimation. Theoretical scaling laws and simulation results consistently show that longer pilots, larger arrays, and stronger received signals improve sensing accuracy, providing practical guidance for pilot and antenna configuration in future ISAC cell-free Massive MIMO deployments.

References

[1] F. Liu, Y. Cui, C. Masouros, J. Xu, T. X. Han, Y. C. Eldar, and S. Buzzi, "Integrated sensing and communications: Toward dual-functional wireless networks for 6G and beyond," *IEEE Journal on Selected Areas in Communications*, vol. 40, no. 6, pp. 1728–1767, 2022.

[2] H. Q. Ngo, A. Ashikhmin, H. Yang, E. G. Larsson, and T. L. Marzetta, "Cell-free massive MIMO versus small cells," *IEEE Transactions on Wireless Communications*, vol. 16, no. 3, pp. 1834–1850, 2017.

[3] Z. Behdad, O. T. Demir, K. W. Sung, E. Bjornson, and C. Cavdar, "Multi-static target detection and power allocation for integrated sensing and communication in cell-free massive MIMO," *IEEE Transactions on Wireless Communications*, vol. 23, no. 9, pp. 11 580–11 596, 2024.

[4] X. Yang, Z. Wei, J. Xu, Y. Fang, H. Wu, and Z. Feng, "Coordinated transmit beamforming for networked ISAC with imperfect CSI and time synchronization," *IEEE Transactions on Wireless Communications*, vol. 23, no. 12, pp. 18 019–18 035, 2024.

[5] F. Liu, T. Zhang, Z. Zhang, B. Cao, Y. Shen, and Q. Zhang, "Fundamental limits of pulse-based UWB ISAC systems: A parameter estimation perspective," *IEEE Internet of Things Journal*, vol. 12, no. 23, pp. 49 387–49 401, 2025.
[6] W. Li, M. Li, M.-M. Zhao, and A. Liu, "Transmit beamforming optimization for cell-free integrated sensing and communication systems," *IEEE Transactions on Wireless Communications*, vol. 25, pp. 1062–1077, 2026.
[7] R. Niu and P. K. Varshney, "Target location estimation in sensor networks with quantized data," *IEEE Transactions on Signal Processing*, vol. 54, no. 12, pp. 4519–4528, 2006.
[8] M. J. Wainwright, "Sharp thresholds for high-dimensional and noisy sparsity recovery using ℓ_1 -constrained quadratic programming (Lasso)," *IEEE Transactions on Information Theory*, vol. 55, no. 5, pp. 2183–2202, 2009.
[9] ——, *High-Dimensional Statistics: A Non-Asymptotic Viewpoint*, ser. Cambridge Series in Statistical and Probabilistic Mathematics. Cambridge: Cambridge University Press, 2019.
[10] X. Zhang and G. Pang, "Fisher-information/CRLB analyses for CF/m-MIMO-AP jointly optimized ISAC networks."
[11] P. Stoica and A. Nehorai, "MUSIC, maximum likelihood, and Cramer-Rao bound," *IEEE Transactions on Acoustics, Speech, and Signal Processing*, vol. 37, no. 5, pp. 720–741, 1989.
[12] Y. Shen, H. Wymeersch, and M. Z. Win, "Fundamental limits of wideband cooperative localization via Fisher information," in *2007 IEEE Wireless Communications and Networking Conference*, 2007, pp. 3951–3955.
[13] D. V. Ouellette, "Schur complements and statistics," *Linear Algebra and its Applications*, vol. 36, pp. 187–295, 1981.
[14] L. P. Barnes and A. Özgür, "Fisher information and mutual information constraints," in *2021 IEEE International Symposium on Information Theory (ISIT)*, 2021, pp. 2179–2184.
[15] L. John Wiley & Sons, *Entropy, Relative Entropy, and Mutual Information*. John Wiley & Sons, Inc., 2005.

APPENDIX A
PROOF OF THEOREM 1

Proof: We proceed with the proof through **Claim 1**, **Claim 2**, and **Claim 3**, respectively, as follows:

Claim 1: To obtain a sub-Gaussian parameter uniform over all directions $\mathbf{u}$, a simple choice for N is

$$N^2 = \lambda_{\max}\left(\mathbf{I}_{\mathbf{x}_{\mathrm{C}}}(\Theta)\right). \tag{60}$$

We use the maximum eigenvalue because it captures the dominant variability/information direction of the matrix, providing a conservative direction-independent measure of correlation strength; since both the correlation matrix and the FIM are built from quadratic outer-product terms, their largest eigenvalues represent the dominant correlation/information mode. For each (m,t), the useful signal can be written as

$$\boldsymbol{\mu}_{m,t}(\boldsymbol{\theta}_m) = \alpha_m \mathbf{a}_m(\phi_m) s_{m,t}. \tag{61}$$

For the real parameter vector $[\alpha_{m,R}, \alpha_{m,I}, \phi_m]^{\mathsf{T}}$, the corresponding derivatives are

$$\begin{cases} \dfrac{\partial \boldsymbol{\mu}_{m,t}}{\partial \alpha_{m,R}} = \mathbf{a}_m(\phi_m) s_{m,t}, \\ \dfrac{\partial \boldsymbol{\mu}_{m,t}}{\partial \alpha_{m,I}} = j\mathbf{a}_m(\phi_m) s_{m,t}, \\ \dfrac{\partial \boldsymbol{\mu}_{m,t}}{\partial \phi_m} = \alpha_m \mathbf{a}'_m(\phi_m) s_{m,t}. \end{cases} \tag{62}$$

Define the Jacobian matrix

$$\mathbf{J}_{m,t}(\boldsymbol{\theta}_m) = \left[\frac{\partial \boldsymbol{\mu}_{m,t}}{\partial \alpha_{m,R}}, \frac{\partial \boldsymbol{\mu}_{m,t}}{\partial \alpha_{m,I}}, \frac{\partial \boldsymbol{\mu}_{m,t}}{\partial \phi_m}\right] \in \mathbb{C}^{L\times 3}. \tag{63}$$

For the model $\mathbf{x}_{m,t} \sim \mathcal{CN}\left(\boldsymbol{\mu}_{m,t}(\boldsymbol{\theta}_m), \sigma^2 \mathbf{I}_L\right)$, the FIM associated with (m,t) satisfies

$$\lambda_{\max}\left(\mathbf{I}_{m,t}(\boldsymbol{\theta}_m)\right) \le \frac{2}{\sigma^2}\left\|\mathbf{J}_{m,t}(\boldsymbol{\theta}_m)\right\|_2^2, \tag{64}$$

where

$$\begin{aligned}\left\|\mathbf{J}_{m,t}(\boldsymbol{\theta}_m)\right\|_2^2 \triangleq{}& \left\|\mathbf{a}_m(\phi_m)s_{m,t}\right\|_2^2 + \left\|j\mathbf{a}_m(\phi_m)s_{m,t}\right\|_2^2 \\ &+ \left\|\alpha_m \mathbf{a}'_m(\phi_m)s_{m,t}\right\|_2^2. \end{aligned}\tag{65}$$

Under the unit-norm/unit-power assumptions $\left\|\mathbf{a}_m(\phi_m)\right\|_2^2 = 1$ and $\left|s_{m,t}\right|^2 = 1$, we obtain

$$\lambda_{\max}\left(\mathbf{I}_{m,t}(\boldsymbol{\theta}_m)\right) \le \frac{2}{\sigma^2}\left(2 + \left|\alpha_m\right|^2 \left\|\mathbf{a}'_m(\phi_m)\right\|_2^2\right). \tag{66}$$

By independence across (m,t), the FIM is additive, i.e.,

$$\mathbf{I}_{\mathbf{x}_{\mathrm{C}}}(\Theta) = \sum_{m=1}^{M}\sum_{t=1}^{T} \mathbf{I}_{m,t}(\boldsymbol{\theta}_m). \tag{67}$$

Hence,

$$\begin{aligned}\lambda_{\max}\left(\mathbf{I}_{\mathbf{x}_{\mathrm{C}}}(\Theta)\right) &\le \sum_{m=1}^{M}\sum_{t=1}^{T} \lambda_{\max}\left(\mathbf{I}_{m,t}(\boldsymbol{\theta}_m)\right) \\ &\le \frac{2MT}{\sigma^2}\left(2 + \left|\alpha\right|^2 \left\|\mathbf{a}'(\phi)\right\|_2^2\right). \end{aligned}\tag{68}$$

Substituting Eq. (60) into Eq. (68) gives

$$N^2 \le \frac{2MT}{\sigma^2}\left(2 + \left|\alpha\right|^2 \left\|\mathbf{a}'(\phi)\right\|_2^2\right), \tag{69}$$

According to [14],

$$\mathsf{Tr}\left(\mathbf{I}_{\mathbf{x}_{\mathrm{C}}}(\Theta)\right) \le 2N^2 \mathcal{I}_{\Theta}\left(\mathbf{x}_{\mathrm{C}}; \mathbf{s}_{\mathrm{C}}\right). \tag{70}$$

Thus, Claim 1 follows.

Claim 2: For the unit-norm ULA steering vector, the l-th entry is

$$a_l(\phi_m) = \frac{1}{\sqrt{L}} e^{j\kappa l \sin\phi_m}, \quad l = 0, \ldots, L-1. \tag{71}$$

Taking the derivative with respect to ϕ_m yields

$$\frac{\partial a_l}{\partial \phi_m} = \frac{1}{\sqrt{L}} e^{j\kappa l \sin\phi_m}\left(j\kappa l \cos\phi_m\right). \tag{72}$$

Therefore,

$$\left\|\mathbf{a}'(\phi_m)\right\|_2^2 = \sum_{l=0}^{L-1}\left|\frac{\partial a_l}{\partial \phi_m}\right|^2 = \frac{1}{L}\kappa^2 \cos^2(\phi_m)\sum_{l=0}^{L-1} l^2. \tag{73}$$

Moreover, $\sum_{l=0}^{L-1} l^2 = \frac{(L-1)L(2L-1)}{6}$, and hence

$$\left\|\mathbf{a}'(\phi_m)\right\|_2^2 = \kappa^2\left(\cos^2\phi_m\right)\left[\frac{(L-1)(2L-1)}{6}\right]. \tag{74}$$

Substituting Eq. (74) into Eq. (20) proves Claim 2.

Claim 3: Since all pilot symbols are equiprobable, the mutual information between $\mathbf{x}_{\mathrm{C}}$ and $\mathbf{s}_{\mathrm{C}}$ satisfies [15]

$$\mathcal{I}_{\Theta}\left(\mathbf{x}_{\mathrm{C}};\mathbf{s}_{\mathrm{C}}\right)\leq H\left(\mathbf{s}_{\mathrm{C}}\right)\leq B_{\mathrm{tot}}, \tag{75}$$

where $B_{\mathrm{tot}}=2bMLT$ is the total number of bits. Substituting Eq. (75) into Eq. (21) proves Claim 3. ∎

APPENDIX B
PROOF OF THEOREM 2

Proof: This appendix derives the local FIM and the auxiliary ULA identities used in Section III. For the Gaussian observation model, the per-pilot local FIM is

$$\mathbf{I}_{m,t}(\boldsymbol{\theta}_m)=\frac{2}{\sigma^2}\Re\{\mathbf{J}_{m,t}(\boldsymbol{\theta}_m)^{\mathsf{H}}\mathbf{J}_{m,t}(\boldsymbol{\theta}_m)\}. \tag{76}$$

Using Eq. (33), $\|\mathbf{a}_m(\phi_m)\|_2^2=1$, and $\mathbb{E}\left[|s_{m,t}|^2\right]=1$, we obtain

$$\mathbf{I}_{m,t}(\boldsymbol{\theta}_m)=\frac{2}{\sigma^2}\begin{bmatrix}1 & 0 & \Re\{\alpha_m q_m\}\\ 0 & 1 & \Re\{-j\alpha_m q_m\}\\ \Re\{\alpha_m q_m\} & \Re\{-j\alpha_m q_m\} & |\alpha_m|^2\eta_m\end{bmatrix}. \tag{77}$$

Summing over the T independent pilots gives

$$\begin{aligned}\mathbf{I}_m(\boldsymbol{\theta}_m)=&\sum_{t=1}^{T}\mathbf{I}_{m,t}(\boldsymbol{\theta}_m)\\ =&\frac{2T}{\sigma^2}\begin{bmatrix}1 & 0 & \Re\{\alpha_m q_m\}\\ 0 & 1 & \Re\{-j\alpha_m q_m\}\\ \Re\{\alpha_m q_m\} & \Re\{-j\alpha_m q_m\} & |\alpha_m|^2\eta_m\end{bmatrix}.\end{aligned} \tag{78}$$

From Eq. (1),

$$\begin{cases}q_m=j\kappa\left(\cos\phi_m\right)\dfrac{L-1}{2},\\ \eta_m=\kappa^2\left(\cos^2\phi_m\right)\dfrac{(L-1)(2L-1)}{6}.\end{cases} \tag{79}$$

Since $q_m=jc_m$, we have $\Re\{\alpha_m q_m\}=-c_m\alpha_{m,I}$ and $\Re\{-j\alpha_m q_m\}=c_m\alpha_{m,R}$, which gives Eq. (36). Moreover,

$$\begin{aligned}\eta_m-c_m^2=&\kappa^2\left(\cos^2\phi_m\right)\left[\frac{(L-1)(2L-1)}{6}-\frac{(L-1)^2}{4}\right]\\ =&\kappa^2\left(\cos^2\phi_m\right)\frac{L^2-1}{12},\end{aligned} \tag{80}$$

which gives Eq. (35). This completes the proof details used by Theorem 2. ∎